

Magnonic-Crystal Waveguides of Width-Modulated Thin-Film Nanostrip Applicable to Broad-Band-Microwave Spin-Wave Filter

Ki-Suk Lee, Dong-Soo Han, and Sang-Koog Kim*

*Research Center for Spin Dynamics & Spin-Wave Devices and Nanospinics Laboratory,
Department of Materials Science and Engineering, College of Engineering,
Seoul National University, Seoul 151-744, Republic of Korea*

We propose, on the basis of micromagnetic modeling and theoretical calculation, a novel planar structure of magnonic-crystal waveguides in which the allowed and forbidden bands of propagating dipolar-exchange spin-waves can be manipulated simply by means of the periodic modulation of different widths in thin-film nanostrips made of a single magnetic material. The periodic width modulation and its periodicity in the nanostrips are crucial parameters for controlling spin-wave band gaps on the order of ~ 10 GHz. A new type of magnonic crystals composed of combinations of differently strip-width modulated nanostrips in series represents a route to the realization of broad-band spin-wave filters in the high-frequency range above ~ 10 GHz.

Over the past decade, photonic crystals [1] have been a hot topic in the research fields of condensed matter physics and optics, owing to their various applications to optical nano-devices such as photonic waveguides [2] and integrated circuits [3]. Meanwhile, in the research areas of nanomagnetism and magnetization (**M**) dynamics, the magnetic counterpart of the photonic crystals, the so-called magnonic crystal (MC), also is a subject of growing interest, owing to its applications to spin-wave (SW) devices such as waveguides and filters [4]. In recent years, many theoretical and experimental studies have been conducted on not only various types of MCs including one-dimensional (1D) structures such as periodic multilayers [5,6], periodic arrays of nanostrips [7], corrugated films [8,9], and comb-like [10] or serial loop structures [11], but also 2D or 3D structures [12,13,14]. In such structures, the allowed and forbidden SW modes (called magnons) are controllable by means of the artificial periodic structure of magnetic media having different magnetic properties, such as magnetic material parameters [5,6,15], shape [8,9,10,11] and exchange-biased field [16]. Despite recent advances in fundamental understandings of those MCs as well as the wave properties of excited SW modes, few studies have been carried out on simple structures of MC waveguides for practical applications to broad-band SW filters. Very recently, it has been demonstrated experimentally that 20 ~ 40 MHz-wide band gaps of magnetostatic SWs can be controlled by means of periodic shallow grooves (of a few tens of μm width and a few hundreds of nm depth) etched on yttrium iron garnet film [9]. However, for future SW-based signal process devices [17,18], it is

necessary to find a few micrometer-scaled MC waveguides having wide band gaps (of a few GHz) for dipolar-exchange spin-waves (DESWs) in laterally confined planar structures.

In this Letter, we propose a new type of simple planar-patterned thin-film nanostrip MC waveguide in which DESW magnonic bands with wide band-gap widths on the order of 10 GHz can be manipulated by means of the periodic modulation of different widths (of a few tens of nm). The relations of the allowed DESW modes and their band gaps to the geometric variation of the proposed MCs were found from micromagnetic numerical and analytical calculations.

We performed micromagnetic simulations of DESW propagations in magnetic thin-film nanostrips. We used, as a model system, 10 nm-thick Py nanostrips of different widths (24 and 30 nm) modulating with a periodicity P ranging from 12 to 42 nm [the light-gray area in Fig. 1(a)], which were connected directly to a segment of the Py nanostrip of 10 nm thickness and 30 nm width [the yellow area in Fig. 1(a)]. The unit period of the nanostrips consists of the same Py segments with the different widths of 24 and 30 nm and with the corresponding lengths P_1 and P_2 , respectively, as illustrated in Fig. 1(b). The OOMMF code [19] was used to numerically calculate the dynamics of the \mathbf{M}_s of individual unit cells (size: $1.5 \times 1.5 \times 10 \text{ nm}^3$) interacting through exchange and dipolar forces, which code uses the Landau-Lifshitz-Gilbert equation of motion [20] valid for temporal scales above 10 ps. The chosen material parameters corresponding to Py are as follows: the saturation magnetization $M_s = 8.6 \times 10^5 \text{ A/m}$, the

exchange stiffness $A_{\text{ex}} = 1.3 \times 10^{-11}$ J/m, the damping constant $\alpha = 0.01$, the gyromagnetic ratio $\gamma = 2.21 \times 10^5$ m/As, with zero magnetocrystalline anisotropy. For the local excitation and subsequent propagation of the lowest DESW mode in the width direction (the y -axis), the so-called plane-wavelike mode in the frequency range of $f_{\text{SW}} = 0 \sim 100$ GHz, we applied a “sine cardinal (sinc)” function, denoted $H_y(t) = H_0 \frac{\sin[2\pi\nu_{\text{H}}(t-t_0)]}{2\pi\nu_{\text{H}}(t-t_0)}$, with $H_0 = 1.0$ T and the field frequency $\nu_{\text{H}} = 100$ GHz in the local area of 1.5×30 nm² indicated by the dark-brown color in Fig. 1(a).

The results obtained by the fast Fourier transform (FFT) of the temporal M_z/M_s evolution are plotted, in Fig. 2, along the x -axis at $y = 15$ nm [18]. The frequency spectra clearly reveal the allowed and/or forbidden bands of the DESWs propagating through the nanostrips: the allowed bands are indicated by the colored region, and the forbidden bands, by the blank or white region. For comparison, the fundamental DESW modes propagating in single-width (24 and 30 nm) nanostrip waveguides are shown in Figs. 2(a) and 2(b). Obviously, there is no forbidden band except for the intrinsic potential barrier (14 GHz), owing to the quantization of the lowest DESW mode by the geometric confinement of the narrow strip width [18,21]. For the differently width-modulated nanostrips, by contrast, it is found that there are several wide forbidden bands on the order of ~ 10 GHz. Moreover, the number of forbidden bands as well as the bands' position and gap width differ according not only to P but also the motif (represented by P_1/P). For example, for $P = 18$ nm ($[P_1, P_2] = [9 \text{ nm}, 9 \text{ nm}]$), there are two

wide band gaps (11 and 16 GHz) in the DESW modes ranging from 14 to 100 GHz, whereas, for $P = 30$ nm ($[P_1, P_2] = [15$ nm, 15 nm]), there are five forbidden bands with smaller gap widths (3.8 ~ 8.6 GHz) (for more data, see Suppl. Fig. 1 [22]).

To comprehensively understand such striking band-gap variations, we plot the dispersion curves of the DESW modes in the 24 and 30 nm-wide nanostrips and in the nanostrip of $[P_1, P_2] = [9$ nm, 9 nm] [23] as an example. Due to the pinning of the DESWs at the edges of the nanostrip width, there exist certain width-modes having quantized k_y values [21]. Generally, in single-width nanostrips, several width-modes are excited and, thus, several concave branches appear in the dispersion curves [18]. In the present simulation, however, there was a single parabolic dispersion curve, as shown in Fig. 3(a), because our employed homogeneous DESW excitations along the width axis led to only the lowest mode having the smallest k_y value [the plane-wavelike mode, see Fig. 1(c)]. Accordingly, one would expect that the dispersion curves for the width-modulated nanostrips be folded and have band gaps at the Brillouin zone (BZ) boundaries, similar to those found typically in a 1D periodic system [2,24]. However, the dispersion curves of the $[P_1, P_2] = [9$ nm, 9 nm] width-modulated nanostrip [Fig. 3(b)] show fairly complicated band features: The band gaps occur not only at the BZ boundaries, $k_x = n\pi/P$ with integers n (black dashed lines), but also at certain k values, $k_x = [(2n+1)\pi \pm 1.44]/P$ (red dotted lines). The former can be explained by a periodic

translation symmetry associated with the width modulation along the DESW propagation direction, but the latter cannot be understood by such a 1D approach.

In order to quantitatively elucidate the physical origin of such different band gaps varying with different strip-width modulation, we compared magnonic band diagrams [the thick black lines in Fig. 4 (a)] numerically obtained from micromagnetic simulations for $[P_1, P_2] = [9 \text{ nm}, 9 \text{ nm}]$, combined with the analytical calculation of the band structure of a single-width (27 nm) nanostrip. Note that this width is the average of the 24 and 30 nm widths of the width-modulated nanostrips. For a single-width nanostrip, the dispersion relation can be approximately expressed as [18,21]

$$\omega_m^2(k_x) = \left[\omega_H + \omega_M L_e^2 \kappa_m^2 + \omega_M f(\kappa_m L) k_{y,m}^2 / \kappa_m^2 \right] \left[\omega_H + \omega_M L_e^2 \kappa_m^2 + \omega_M \{1 - f(\kappa_m L)\} \right] \quad (1)$$

with $f(\kappa_m L) = 1 - [1 - \exp(-x)]/x$, where $\omega_H = \gamma H_{\text{in}}$ with internal field H_{in} , $\omega_M = 4\pi\gamma M_s$, $L_e = \sqrt{A_{\text{ex}} / (2\pi M_s^2)}$ is the exchange length, and $\kappa_m^2 = k_x^2 + k_{y,m}^2$ is the in-plane-wave vector. The quantized $k_{y,m}$ can be obtained by considering the ‘‘effective’’ pinning [18,21] for a given single-width nanostrip, for example, $k_{y,m} = m \times 0.072 \text{ nm}^{-1}$ for a 27 nm-width nanostrip. In Fig. 4(a), the solid red line indicates the dispersion curves of the DESW mode with $m = 1$, the lowest mode excited. Owing to the periodicity of the width modulation, the dispersion curves are folded at the first BZ boundary (the dashed vertical line), as shown in Fig. 4(a), and thus, these folded branches intersect with the original one at the BZ boundaries. Such a crossing of dispersion curves indicates the ‘diagonal’ coupling between the two identical modes having

opposite propagation vectors [25], that is, it denotes the interference between the initially propagating forward mode and the backward mode reflected at the BZ boundary. This diagonal coupling results in the formation of a standing DESW wave pattern with $k_x = n\pi/P$ in the MC of P , and yields a split in the energy band (a band gap) [see the thick black lines in Fig. 4(a)] [24].

To obtain the standing wave profiles near each band edge, we calculated the spatial distributions of the FFT powers of the local M_z/M_s oscillations for the indicated specific frequencies selected at the top and bottom of the magnonic band for the case of $[P_1, P_2] = [9 \text{ nm}, 9 \text{ nm}]$, as shown in Fig. 4(b). From the FFT profiles for the first band gap [26], it was verified that the origin of the first band gap is the plane-wavelike standing wave modes [see the cross-sectional profile in Fig. 4(c)] originating from the diagonal coupling between the two identical but oppositely propagating lowest DESW modes ($m = 1$).

Given the multiple 2D scattering (diffraction) of SWs from the short-width edge steps [see Fig. 1(b)], the higher-quantized modes ($m = 3, 5, 7\dots$) [27] can also be excited, though we generated, by applying the homogeneous field in the width direction (y -axis), only the plane-wavelike DESW having the first quantized wave vector ($m = 1$) in the 30 nm-width segment of the width-modulated nanostrip. The dotted orange lines in Fig. 4(a) indicate the dispersion curves of the DESW mode with $m = 3$, which are also folded at the first BZ boundary. Interestingly, this dispersion branch of the higher quantized mode ($m = 3$) excited by the DESW

diffraction intersects with that of the lowest mode ($m = 1$) at certain k values, $k_x = [0.5 \pm 0.2]2\pi/P$, away from the BZ boundaries, as indicated by the blue circles and the arrows in Fig. 4(a). Such an intersection can have a remarkable influence on the propagating DESW modes. In general, SWs scattered from the short-width edge steps propagate in the wide direction on the x - y plane, so that they interfere destructively with themselves. However, for the phase-matching condition of the diffracted SWs, indicated by the intersection points in the dispersion curves shown in Fig. 4(a), these scattered SWs interfere constructively with themselves; in other words, another SW mode ($m = 3$) being propagating in the opposite direction is excited, and interacts with the initial propagating mode. Consequently, their interactions lead to quite complicated 2D standing SW mode: for $f_{\text{SW}} = 66.8$ GHz, the nodes appear in the width direction (y -axis) and along the x -axis [see Figs. 4(b) and 4(c)], subsequently leading to complex 2D normal modes in thin films with lateral confinements [28]. This results in the anti-crossing of dispersion curves as well as band gaps [25] [see the thick black lines for the second and the third bands and the diagonal-line-patterned blue region between them in Fig. 4(a)]. Such strong couplings between the two different modes, and the resulting band gaps are well known as ‘mini-stopbands’ [2,25,29] in photonic-crystal-waveguide electromagnetic waves.

On the basis of such novel DESW band structures, it was found that magnonic band gaps vary sensitively according to both the periodicity and the motif in strip-width-modulated

nanostrips, as seen in Suppl. Fig.2 [22]. From an application point of view, this novel property can be implemented as an effective means of manipulating the allowed DESW modes in their propagations through such width-modulated nanostrip waveguides. Here, we propose a new type of SW waveguide that passes DESWs in a chosen narrow-band frequency region but filters out most DESWs having other frequencies. The proposed width-modulated planar structure, as shown in Fig. 5(a), consists of four different nanostrip segments having different strip-width modulations and different periodicities and repeating numbers. These serially combined nanostrips were designed for passing SWs in the narrow band of 26 ~ 32 GHz, based on the results of the variations of the band gaps with P and P_1 (see Suppl. Fig. 2 [22]). According to the frequency spectrum [Fig. 5(b)], and the transmitted intensity (represented by FFT power) of the DESWs versus the propagation distance [Fig. 5(c)], the narrow-frequency-range (26 ~ 32 GHz) DESWs propagate well with a transmitted intensity of about 10%, even after propagating as far as 1.5 μm , indicating that such MC structures effectively filter out most SWs, except for the chosen SW mode. Another example of a narrow-band SW filter, having a 36 ~ 41 GHz pass band, is shown in Suppl. Fig. 3 [22].

In conclusion, we found that a new type of MC of periodically modulating strip widths yields complex DESW band structures and wide band gaps, originating from the coupling between not only identical modes but also different modes in width-modulated nanostrips. The magnonic band-gap width, the position, and the number of band gaps are controllable by means

of the periodicity and the motif of the strip-width modulation. Moreover, we propose promisingly efficient MC waveguides of serially connected different-width-modulated nanostrip segments for narrow-band-pass DESWs retaining $\sim 10\%$ transmission intensity after propagations as far as $\sim 1 \mu\text{m}$, making possible the realization of SW filters using a simple planar-patterned thin-film structure composed of a single magnetic material.

This work was supported by Creative Research Initiatives (the Research Center for Spin Dynamics and Spin-Wave Devices) of MEST/KOSEF.

References:

* corresponding author, e-mail address: sangkoog@snu.ac.kr

- [1] E. Yablonovitch, Phys. Rev. Lett. **58**, 2059 (1987).
- [2] J. D. Joannopoulos, R. D. Meade, and J. N. Winn, Photonic Crystals: Molding the Flow of Light, 2nd ed. (Princeton University, Princeton, NJ, 2008).
- [3] N. Engheta, Science **317**, 1698 (2007).
- [4] R. L. Carter *et al.*, J. Appl. Phys. **53**, 2655 (1982).
- [5] D. S. Deng, X. F. Jin, and R. Tao, Phys. Rev. B **66**, 104435 (2002).
- [6] S. A. Nikitov, Ph. Tailhades, and C. S. Tsai, J. Magn. Magn. Mater. **236**, 320 (2001).
- [7] M. P. Kostylev, A. A. Stashkevich, and N. A. Sergeeva, Phys. Rev. B **69**, 064408 (2004); M. Kostylev *et al.*, Appl. Phys. Lett. **92** 132504 (2008).
- [8] C. G. Sykes, J. D. Adam, and J. H. Collins, Appl. Phys. Lett. **29**, 388 (1976); P. A. Kolodin and B. Hillebrands, J. Magn. Magn. Mater. **161**, 199 (1996).
- [9] A. V. Chumak *et al.*, Appl. Phys. Lett. **93**, 022508 (2008).
- [10] H. Al-Wahsh *et al.*, Phys. Rev. B **59**, 8709 (1999).
- [11] A. Mir *et al.*, Phys. Rev. B **64**, 224403 (2001).
- [12] J. O. Vasseur *et al.*, Phys. Rev. B **54**, 1043 (1996).
- [13] Yu. V. Gulyaev *et al.*, JETP Lett. **77**, 567 (2003).

- [14] M. Krawczyk and H. Puzskarski, Phys. Rev. B **77**, 054437 (2008).
- [15] V.V. Kruglyak, and R.J. Hicken, J. Magn. Magn. Mater. **306**, 191 (2006); V.V. Kruglyak *et al.*, J. Appl. Phys. **98**, 014304 (2005).
- [16] C. Bayer, M. P. Kostylev, and B. Hillebrands, Appl. Phys. Lett. **88**, 112504 (2006).
- [17] R. Hertel, W. Wulfhekel, and J. Kirschner, Phys. Rev. Lett. **93**, 257202 (2004); T. Schneider *et al.*, Appl. Phys. Lett. **92**, 022505 (2008); K.-S. Lee and S.-K. Kim, J. Appl. Phys. **104**, 053909 (2008).
- [18] S. Choi, K.-S. Lee, K. Y. Guslienko and S.-K. Kim, Phys. Rev. Lett. **98**, 087205 (2007).
- [19] See <http://math.nist.gov/oommf>.
- [20] L. D. Landau and E. M. Lifshitz, Phys. Z. Sowjet. **8**, 153 (1935); T. L. Gilbert, Phys. Rev. **100**, 1243A (1955).
- [21] K. Yu. Guslienko *et al.*, Phys. Rev. B **66**, 132402 (2002); K. Yu. Guslienko and A. N. Slavin, Phys. Rev. B **72**, 014463 (2005).
- [22] See EPAPS Document No. XXX for two movie files. For more information on EPAPS, see <http://www.aip.org/pubservs/epaps.html>.
- [23] Dispersion curves were obtained from the 2D FFTs of the temporal M_z/M_s oscillations along the x -axis ($x = 501 \sim 1500$ nm) at $y = 15$ nm (the dashed line on the nanostrip MC in Fig. 1).
- [24] C. Kittel, Introduction to Solid State Physics, 7th ed. (Wiley, New York, 1996).

[25] J.-M. Lourtioz *et al.*, Photonic Crystals: Towards Nanoscale Photonic Devices (Springer, Berlin, 2005).

[26] The top of the first allowed band ($f_{\text{SW}} = 25.6$ GHz) and the bottom of the second allowed band ($f_{\text{SW}} = 36.4$ GHz) appear at the edge of the Brillouin zone at $k_x = \pi/P$.

[27] Since the edge steps are symmetric with respect to the x -axis (mirror plane), higher-quantized modes have a mirror symmetry in the profiles along the short-width axis; in other words, they have odd-number m values (i.e., $m = 3, 5, 7 \dots$).

[28] M. Grimsditch *et al.*, Phys. Rev. B **69**, 174428 (2004); M. Grimsditch *et al.*, Phys. Rev. B **70**, 054409 (2004).

[29] S. Olivier *et al.*, Phys. Rev. B **63**, 113311 (2001).

Figure captions

FIG. 1. (Color online) (a) Geometry and dimensions of proposed nanostrip MCs with periodic modulation of different strip widths. The initial \mathbf{M} s point in the $-x$ direction, as indicated by the black arrow. The dark-brown and yellow areas indicate the SW generation and the waveguide component of the SW propagation, respectively. (b) The unit period of $P = P_1 + P_2$, where P_1 and P_2 are the segment lengths of 24 and 30 nm widths, respectively. (c) Temporal evolution of spatial M_z/M_s distribution excited by “sinc” function field with $H_0 = 1.0$ T applied along y -axis to only dark-brown area.

FIG. 2. (Color online) Frequency spectra obtained from fast Fourier transform (FFT) of M_z/M_s oscillation along x -axis at $y = 15$ nm, for single-width nanostrips of 24 and 30 nm and for MCs of different $[P_1, P_2]$ noted. The vertical dashed orange lines indicate the boundary between the single-width nanostrip waveguide [the yellow area in Fig. 1(a)] and the MC of the width-modulated nanostrip [the light-gray area in Fig. 1(a)].

FIG. 3. (Color online) (a) Dispersion curves for DESWs propagating through single-width nanostrips of 24 and 30 nm. (b) Dispersion curves of DESWs existing in MCs of $[P_1, P_2] = [9$ nm, 9 nm] within nanostrip area only, from $x = 500$ to 1500 nm, obtained from FFTs of temporal M_z/M_s oscillations along x -axis at $y = 15$ nm. The black dashed lines indicate the

Brillouin zone boundaries $k = n\pi/P$, where $n = 0, \pm 1, \pm 2, \dots$, and the red dotted lines denote certain k values, $k_x = (2n+1)\pi/P \pm 0.08$ at which the forbidden band gaps occur.

FIG. 4. (Color online) (a) Comparison of magnonic band structure (black thick curves) of nanostrip-type MC of $[P_1, P_2] = [9 \text{ nm}, 9 \text{ nm}]$ obtained from micromagnetic simulations and that of single-width nanostrips of 27 nm width, for two different modes of $m = 1$ (solid red) and $m = 3$ (dotted orange) obtained from Eq. (1). (b) Perspective view of FFT power distributions of local M_z/M_s oscillations for specific frequencies for top and bottom of allowed bands, as indicated by orange horizontal lines in dispersion curves shown in Fig. 3(b). (c) Cross-sectional FFT power profiles of standing wave modes in width direction (y -direction). The red (green) line indicates the standing wave mode profile in the width direction at the center of the 30 nm- (24 nm-) wide segment.

FIG. 5. (Color online) (a) Proposed wide-band SW filter in GHz range having only narrow pass band of 26 ~ 32 GHz, and composed of four different strip-width modulations, each of which is represented by $[P_1 \text{ (nm)}, P_2 \text{ (nm)}] = [21, 21], [13.5, 13.5], [12, 12],$ and $[7.5, 7.5]$ in the present case. (b) Frequency spectra along long axis (x -axis) of nanostrip. The vertical lines separate the different period modulations. (c) FFT power profiles along long axis (x -axis) of nanostrip for different frequencies noted.

FIG.1

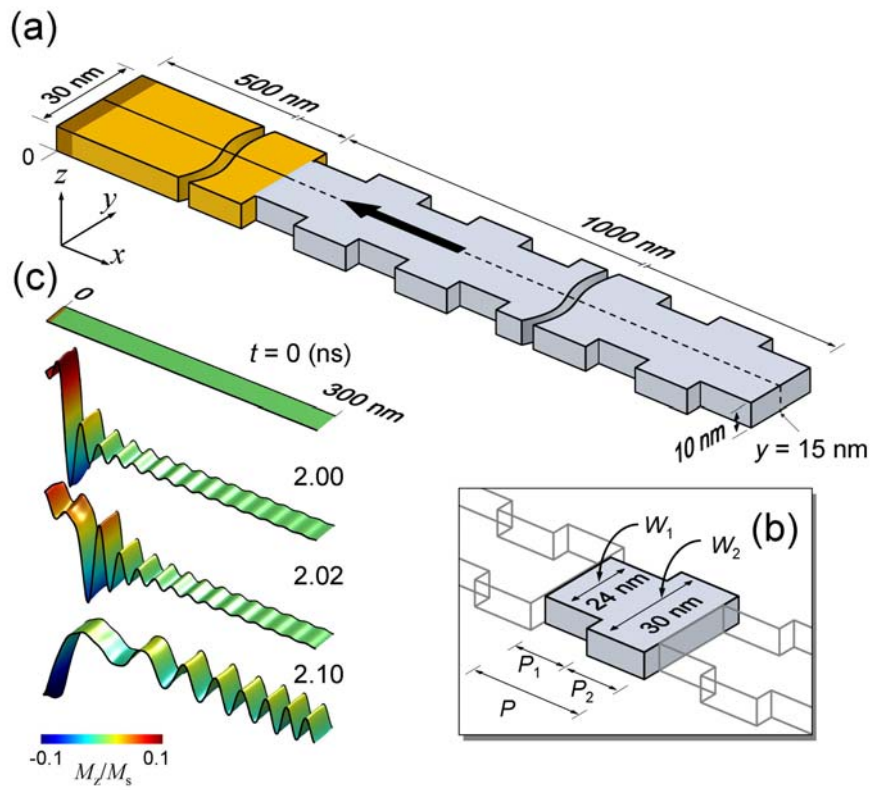


FIG.2

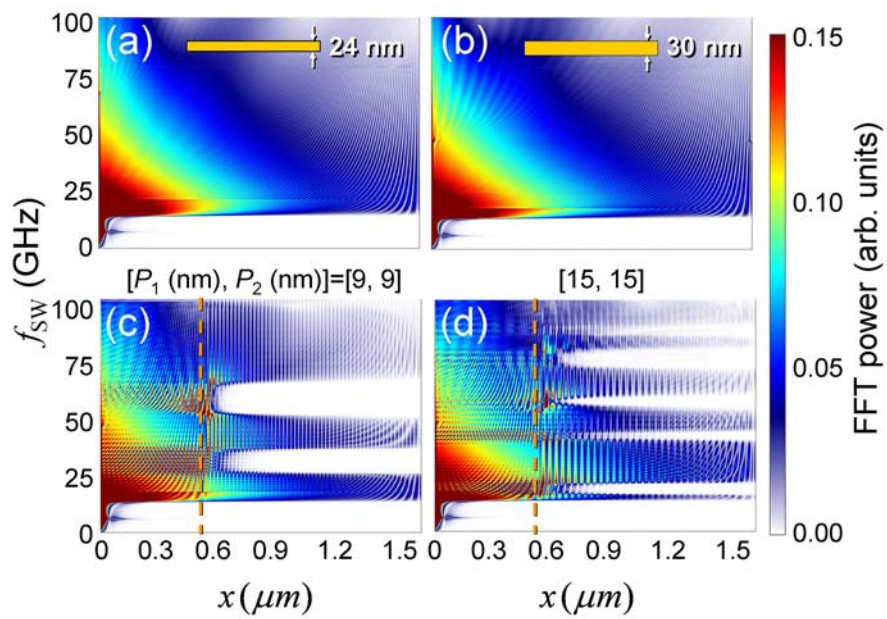


FIG.3

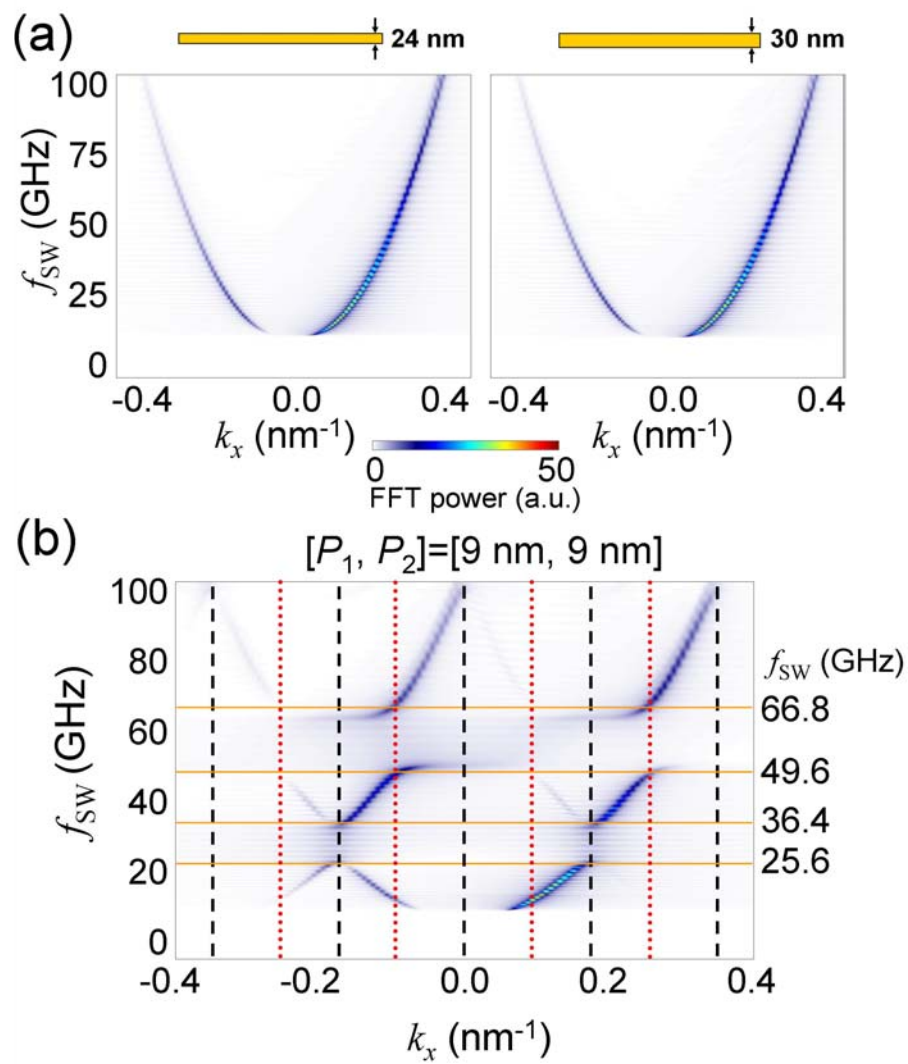


FIG.4

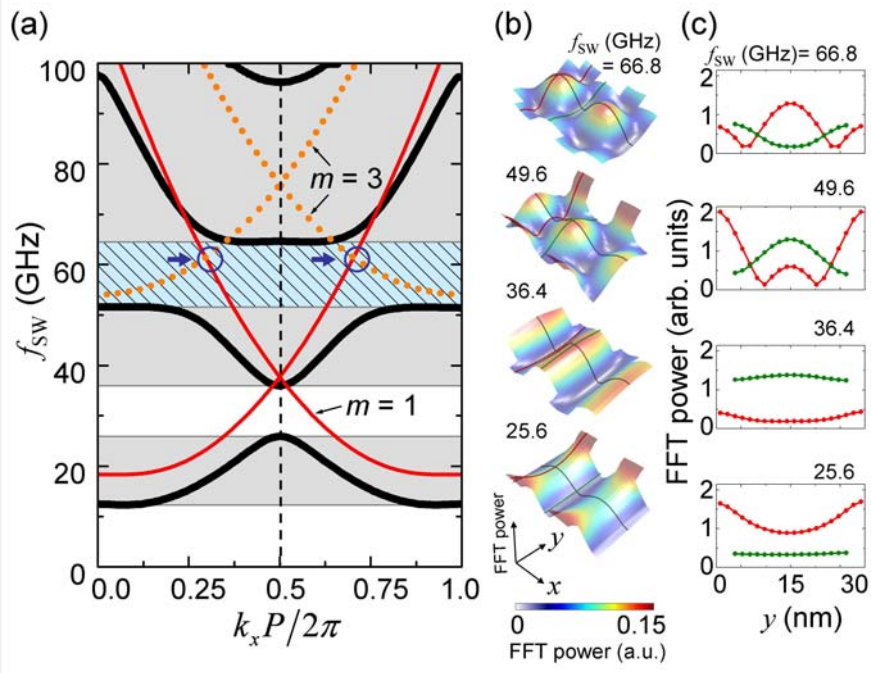
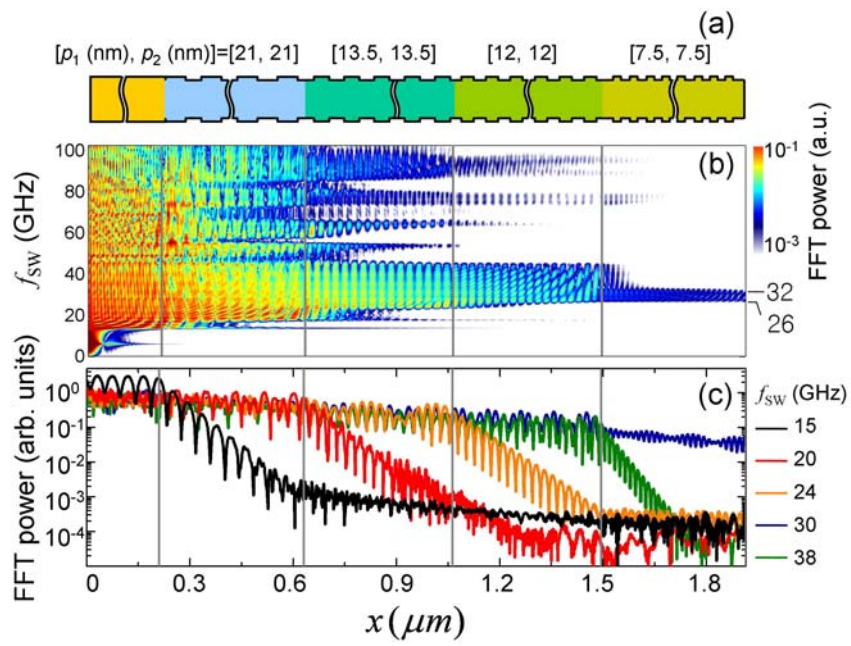


FIG.5

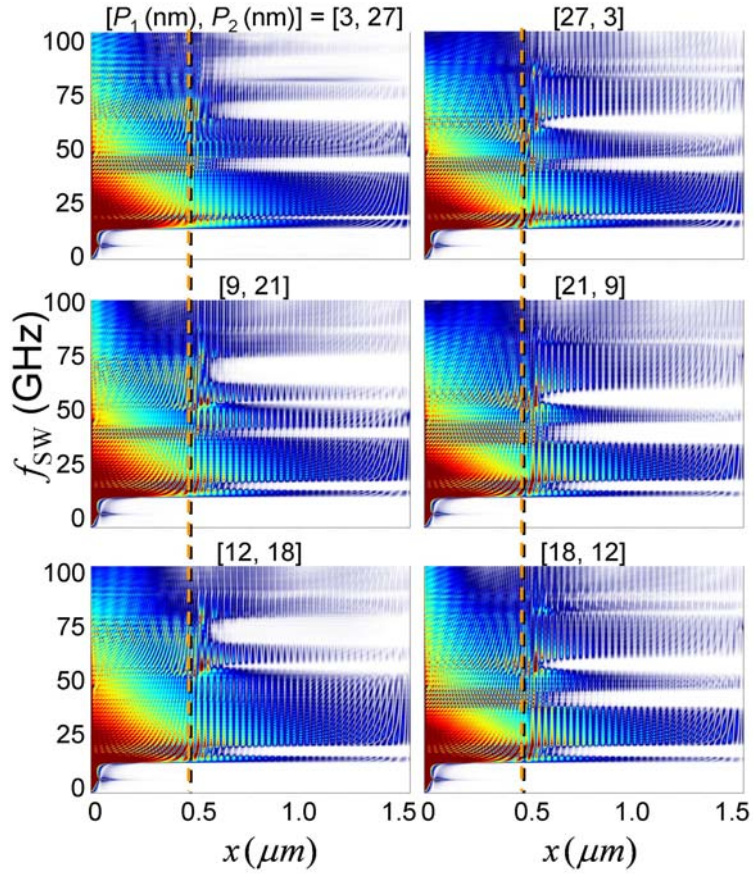


Supplementary Documents

Variation of the allowed and forbidden bands according to periodicity P and motif represented by P_1/P

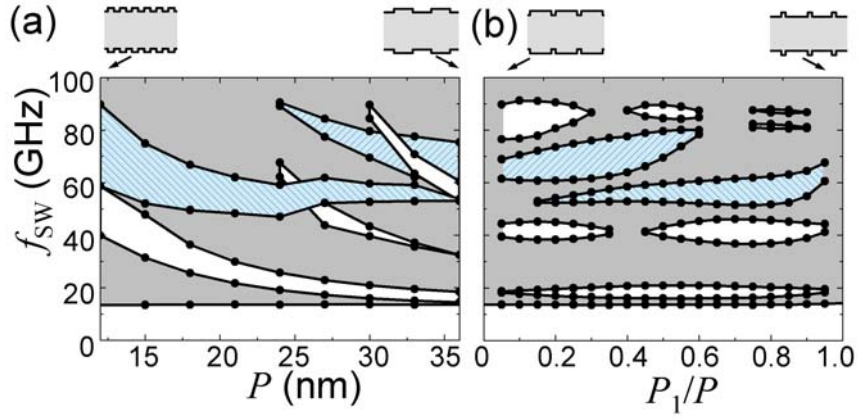
To examine the variation of the allowed and forbidden bands in nanostrip-type magnonic crystals (MCs) according to the periodicity $P = P_1 + P_2$ and the motif represented by the relative segment length, P_1/P , we obtained frequency spectra along the x -axis for various values of P_1 and P_2 , as shown in Suppl. Fig. 1. From these data, the magnonic band gaps were plotted versus P while retaining $P_1 = P_2$ in Suppl. Fig. 2(a), and versus P_1/P with the constant value of $P = 30$ nm in Suppl. Fig. 2(b). All of the gray regions indicate the allowed bands, whereas the white and blue regions indicate the forbidden bands at the zone boundary and at a certain k value away from the zone boundary, respectively. As seen in Suppl. Fig. 2(a), the number of band gaps as well as the center positions and widths of the individual gaps change dramatically with P . For the forbidden bands at the zone boundaries (the white regions), the center position and width of each band decrease with increasing P , whereas the center positions do not change with P_1/P . With regard to the forbidden bands occurring away from the zone boundary (the blue region), by contrast, their center positions change with both P and P_1/P .

SUPPL. FIG. 1



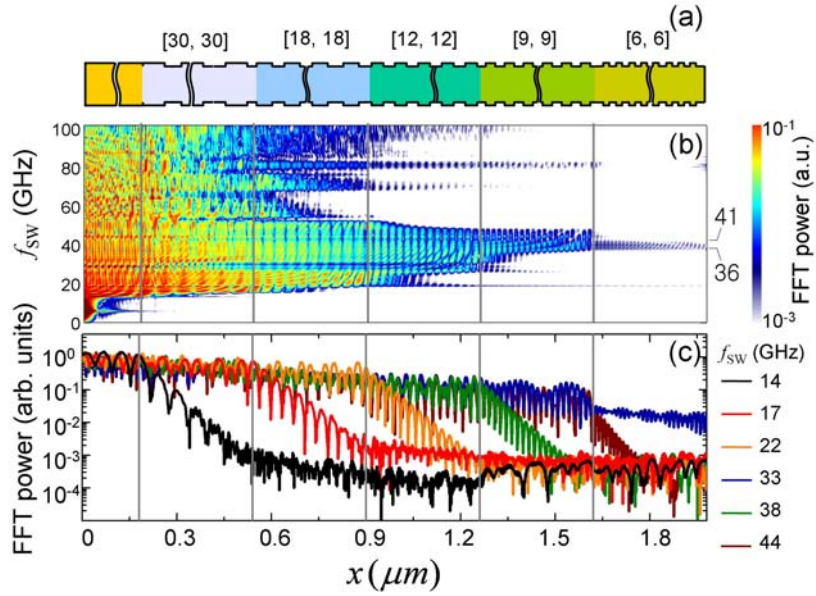
SUPPL. FIG. 1. Frequency spectra obtained from fast Fourier transform (FFT) of M_z/M_s oscillation along x -axis at $y = 15$ nm, for cases of same $P = 30$ nm but different P_1/P values noted. The vertical dashed orange lines indicate the boundary between the single-width nanostrip waveguide [the yellow area in Fig. 1(a)] and the MC of the width-modulated nanostrip [the light-gray area in Fig. 1(b)].

SUPPL. FIG. 2



SUPPL. FIG. 2. Allowed and forbidden bands according to P for the case of $P_1 = P_2$ in (a) and P_1/P , maintaining $P = P_1 + P_2 = 30$ nm in (b). The gray area indicates the allowed bands, whereas the white (blank) and blue (diagonal-line-patterned) areas indicate the forbidden bands at the Brillouin zone boundary $k = n\pi/P$, where $n = 0, \pm 1, \pm 2, \dots$, and certain k values, $k \neq n\pi/P$, respectively.

SUPPL. FIG. 3



SUPPL. FIG. 3. (a) Proposed wide-band SW filter in GHz range having pass band of 36 ~ 41 GHz, and composed of four different strip-width modulations, each of which is represented by $[P_1$ (nm), P_2 (nm)] = [30, 30], [18, 18], [12, 12], [9,9], and [6, 6], in the present case. (b) Frequency spectra along long axis (x -axis) of nanostrip. The vertical lines separate the different period modulations. (c) FFT power profiles along long axis (x -axis) of nanostrip for different frequencies noted.